HENRY

Hydraulic Engineering Repository

Ein Service der Bundesanstalt für Wasserbau

Conference Paper, Published Version

Abdelaziz, Shokry; Bui, Minh-Duc; Rutschmann, Peter

Numerical simulation of scour development due to submerged horizontal jet

Numerical simulation of scour development due to submerged horizontal jet

S. Abdelaziz, M.D. Bui, & P. Rutschmann
Institute of Hydraulic and Water Resources Engineering, Technische Universität München, Munich, Germany

ABSTRACT: A computation module for sediment transport in open channels was developed and incorporated into the commercial code FLOW-3D. In the module, the bed-load transport is simulated with a non-equilibrium model. Effects of bed slop and material sliding are also taken into account. The bed deformation is obtained from an overall mass-balance equation for sediment transport. This paper presents the results of a model application to simulate scour development downstream of an apron due to submerged jet. The bed deformation predictions are compared with measurements, for which the results show generally good agreement compared with experimental data. The model is then used to study the effect of efflux discharges on the bed deformation in the flume.

Keywords: Scour, Sediment Transport, Numerical Modeling

1 INTRODUCTION

Scour downstream of an apron due to submerged jet issuing from a sluice opening is important from the point of view of the stability of hydraulic structures. Accurate prediction of time evolution and ultimate scour depth is necessary to ensure the safety and stability of these structures.

FLOW-3D is a commercial package developed by Flow Science Inc at Los Alamos Scientific Lab. The software uses several special features for numerical solution of the Navier-Stokes equations for free surface flows (VOF-method) and meshing of complicated geometries (FAVOR method). The sediment scour model treats sediment as two concentration fields: the suspended sediment and the packed sediment. The suspended sediment advects and drifts with the fluid due to the influence of the local pressure gradient. Suspended sediment originates from inflow boundaries or from erosion of packed sediment. The packed sediment, which does not advect, represents sediment that is bound by neighboring sediment particles. From the physical point of view, the assumption of the two concentration fields seems to be valid to model fine sediment bed materials. However, for coarse bed materials it could be not correct and we could not get acceptable results in this case. Smith (2007) applied FLOW-3D scour model to fine sediment

transport around a fixed cylinder to predict the bed change with the time. The results show that time scale predictions within the initial stages of scour were in good agreement with the observations. However, predictions of the time scale for the later stages of scour hole development were significantly under predicted. Overall shape of the scour hole was in reasonably good agreement with observations; however the depth of the scour hole was under-predicted. Vasquez and Walsh (2009) applied FLOW-3D to compute the initial stages of scour development in a complex pier made of a large pile cap and 10 cylindrical piles. The results were in qualitative agreement with experimental data. However, additional research using finer grids is needed to quantitatively verify the model. They added also that, the main practical limitation of FLOW-3D and CFD models in general, is computational time. If a very large grid is needed for modeling the structure, computing long-term equilibrium scour may require an exorbitant amount of computational time, much larger than that required for running a physical model.

A computation module for non-cohesive sediment transport in open channels was developed at the Institute of Hydraulic and Water Resources Engineering, Technische Universität München and incorporated into FLOW-3D. In this module, suspended transport is simulated through the gen-

eral convection-diffusion equation with an empirical settling velocity term and the exchange of suspended sediment and bed-load at the lower boundary of the suspended sediment layer. Bed-load transport is simulated with a non-equilibrium model and the bed deformation is obtained from an overall mass-balance equation. In the module, effects of bed slope and bed material sliding on the sediment transport are also taken into account. This paper presents first results of the validation of the developed module for bed-load transport.

2 GOVERNING EQUATIONS

2.1 *Hydrodynamic model*

The hydrodynamic module is based on the solution of the three-dimensional Navier-Stokes equations and the continuity equation. The continuity equation and the model formulation of the Navier-Stokes equations for incompressible flows used in FLOW-3D are as follows (Flow Science Inc., 2008):

$$\frac{\partial}{\partial X_i} U_i A_i = 0 \qquad (1)$$

$$\frac{\partial U_i}{\partial t} + \frac{1}{V_f}\left(U_j A_j \frac{\partial u_i}{\partial X_j}\right) = -\frac{1}{\rho}\frac{\partial P}{\partial X_i} + G_i + f_i \qquad (2)$$

where:

$$\rho V_f f_i = \tau_{b,i} - \left[\frac{\partial}{\partial X_j}\left(A_j S_{ij}\right)\right];$$

$$S_{ii} = -2\mu_{tot}\left[\frac{\partial U_i}{\partial X_i}\right]; \qquad (3)$$

$$S_{ij} = -\mu_{tot}\left[\frac{\partial U_i}{\partial X_j} + \frac{\partial U_j}{\partial X_i}\right].$$

where U_i=mean velocity; P=pressure; A_i=fractional open area open to flow in the i direction; V_f=fractional volume open to flow; G_i represents the body accelerations; f_i represents the viscous accelerations; S_{ij}=strain rate tensor; $\tau_{b,i}$=wall shear stress; ρ=density of water; μ_{tot}=total dynamic viscosity, which includes the effects of turbulence ($\mu_{tot}=\mu+\mu_T$); μ=dynamic viscosity; and μ_T=eddy viscosity.

The wall boundary conditions are evaluated differently based on the chosen turbulence closure scheme. Transport turbulence closure schemes (e.g., k-ε model) use a law of the wall formulation. The combined smooth and rough logarithmic law of the wall equation is iterated in order to solve for the shear velocity u∗ (Flow Science Inc., 2008; Smith et al., 2005):

$$u_o = u_*\left[\frac{1}{\kappa}\ln\left(\frac{\rho u_* y_o}{\mu + \rho a u_* K_s}\right) + 5.0\right] \qquad (4)$$

where κ=von Karman constant; a is a constant, which is equal to 0.247 for k-ε and RNG models, or 0.246 otherwise; k_s is the roughness; and y_0=distance from the solid wall to the location of tangential velocity, u_0. The denominator of Eq. (4) represents an effective viscosity due to the effect of the rough boundary ($\mu_{eff}=\mu+\rho a u_* k_s$). If the cell is within the laminar sublayer ($\rho u_* y_0/\mu \le 5.0$), the solution for the shear velocity is defined with:

$$u_* = \sqrt{\frac{\mu.u_o}{\rho y_o}} \qquad (5)$$

The solution for the shear velocity is used as the wall boundary conditions for the turbulent transport equations (Eq.12).

For laminar flows and non-transport turbulence closure schemes (e.g., LES models), the wall shear stress $\tau_{b,i}$ is defined with

$$\tau_{b,i} = \frac{\left(\mu + \rho a u_o k_s\right) u_o}{y_o} \qquad (6)$$

The model has several different turbulence closure schemes, including one-equation turbulent energy (k), two-equation (k-ε), renormalization-group (RNG), and large eddy simulation (LES) closure schemes. The k-ε closure scheme will be considered as the transport closure scheme in this paper. The standard k-ε model (Wilcox 2000) approximates the eddy viscosity with

$$\mu_T = \frac{\rho C_\mu k^2}{\varepsilon} \qquad (7)$$

The closure equations for the turbulent kinetic energy, k, and the dissipation rate, ε, are given by

$$\frac{\partial k}{\partial t} + \frac{1}{V_f} U_i A_{xi} \frac{\partial k}{\partial X_i} = C_{sp}\frac{\mu}{\rho V_f}\left\{2A_{xi}\left(\frac{\partial U_i}{\partial X_i}\right)^2\right.$$

$$+\left(\frac{\partial U_i}{\partial X_j} + \frac{\partial U_j}{\partial X_i}\right)\left(A_{xj}\frac{\partial U_i}{\partial X_j} + A_{xi}\frac{\partial U_j}{\partial X_j}\right)\right\} - \qquad (8)$$

$$\frac{1}{V_f}\frac{\partial}{\partial X_j}\left[\frac{A_{xi}}{\rho}\left(\mu + \frac{\mu_T}{\sigma_k}\right)\frac{\partial k}{\partial X_j}\right]$$

where C_{sp} is the shear production coefficient.

$$\frac{\partial \varepsilon}{\partial t} + \frac{1}{V_f} U_i A_{xi} \frac{\partial \varepsilon}{\partial x_i} = C_{\varepsilon 1} \frac{\varepsilon}{k} \left(C_{sp} \frac{\mu}{\rho V_f} \left(2 A_{xi} \left(\frac{\partial U_i}{\partial X_i} \right)^2 \right. \right.$$

$$\left. + \left(\frac{\partial U_i}{\partial X_j} + \frac{\partial U_j}{\partial X_i} \right) \left(A_{xj} \frac{\partial U_i}{\partial X_j} + A_{xi} \frac{\partial U_j}{\partial X_i} \right) \right) -$$

$$\frac{1}{V_f} \frac{\partial}{\partial X_j} \left[\frac{A_{xi}}{\rho} \left(\mu + \frac{\mu_T}{\sigma_k} \right) \frac{\partial k}{\partial X_j} \right] - C_{\varepsilon 2} \frac{\varepsilon^2}{k}$$

$$(9)$$

The closure coefficients and auxiliary relations are $C_{\varepsilon 1} = 1.44$, $C_{\varepsilon 2} = 1.92$, $C_\mu = 0.09$, $\sigma_k = 1.0$, $\sigma_\varepsilon = 1.3$

The Reynolds-stress tensor, τ_{ij}, and the mean strain-rate tensor, e_{ij}, are defined with

$$\tau_{ij} = 2 \frac{\mu_T}{\rho} e_{ij} - \frac{2}{3} k \delta_{ij} \qquad (10)$$

$$e_{ij} = \frac{1}{2} \left(\frac{\partial U_i}{\partial Xj} + \frac{\partial U_j}{\partial X_i} \right) \qquad (11)$$

The boundary conditions for k and ε are computed using the logarithmic law of the wall formulation and are defined with

$$k = \frac{u_*^2}{\sqrt{C_\mu}}; \varepsilon = \frac{u_*^3}{\kappa y_o} \qquad (12)$$

FLOW-3D handles free surfaces using a method known as the Volume of Fluid (VOF) technique pioneered by Hirt and Nichols (1981). This technique consists of three components: a method for finding the free surface, an algorithm for tracking the free surface as a sharp interface moving through the computational mesh and a process for applying boundary conditions to the surface. The method uses the simple principle of assigning a single variable F (fluid fraction) to each cell that has a value of 1.0 if the cell is occupied by fluid and a value of 0.0 if the cell is completely empty. Therefore, if the cell has a value of F between 0.0 and 1.0 then the cell contains a free surface. In addition, the normal to the surface can be calculated from the direction in which F changes most rapidly applying boundary conditions to the surface.

FLOW-3D permits the modeling of complicated geometries by allowing the partial blockage of each cell in a regular mesh. The partial blockage of mesh cells is represented by associating a single volume fraction (V_F) and three area fractions (AFR, AFB, and AFT) with each computational mesh cell. The volume fraction is the frac-

tion of the cell volume which may be occupied by fluid. It is, therefore, one minus the fraction of the cell volume which is occupied by solid material. The area fractions are defined as the fraction of the area of each mesh cell face through which fluid may flow. Those associated with a particular cell are the faces between it and the next higher cell in the x (AFR), y (AFB), and z (AFT) directions. The other three faces of a particular cell have area fractions that are associated with the next lower cell in each direction. (Sicilian, 1990)

2.2 FLOW-3D scour model

The FLOW-3D scour module uses a bulk approximation of a conservation of mass and advection/diffusion scheme to predict the transport of sediment. The drift and settling length scale (L_{drift}) of the suspended sediment is calculated using a Stokes formulation at the hydrodynamic time step (Brethour, 2003):

$$L_{drift} = \frac{d_{50}^2}{18\mu} \frac{\nabla P}{\overline{\rho}} (\rho_s - \rho) \Delta t \qquad (13)$$

where ρ_s is the sediment density; ρ is the density of the fluid; d_{50} is the median grain size; Δt is time step. In this case, acceleration is represented by the mechanical gradient $(\Delta P / \overline{\rho})$. Physically, the drift is assumed to be a result of the particle forcing due to gravity and advection. The local density $\overline{\rho}$ is given by:

$$\overline{\rho} = \rho + f_s (\rho_s - \rho) \qquad (14)$$

where f_s is the solid fraction in the cell.
The lift length of the packed bed is calculated using an excess shear formulation:

$$L_{lift} = \overline{n_s} \alpha \sqrt{\frac{\tau - \tau_{cr}}{\overline{\rho}}} \Delta t \qquad (15)$$

where τ_{cr} is the critical shear stress; n_s is the unit vector normal to the bed. The lift acts perpendicular to the bed. The parameter is dimensionless and represents the probability that a particle is lifted from the bed.
The scour module continually provides feedback to the hydrodynamic solver by using an enhanced viscosity for the suspended sediment and a drag term to parameterize inter-granular collisions for the packed bed. These equations are given below.

$$\mu_* = \mu \left(1 - \frac{\min(f_s, f_{s,co})}{f_{s,cr}} \right) \qquad (16)$$

where f_s is the solid fraction in the cell. The solid fraction is a measure of the fraction of the cell vo-

lume that is occupied by sediments. The term $f_{s,co}$ represents the cohesive solid fraction, which is the value at which the sediment particles start to interact with each other. This can also be thought of as the lower bed load limit. The term $f_{s,cr}$ represents the critical solid fraction, or bed porosity. This value corresponds to the point at which the bed material is bound together and acts like a solid mass. When the solid fraction exceeds the cohesive solid fraction, viscosity is no longer enhanced.

2.3 Bed-load transport module

The bed level change z_b is calculated from the overall mass balance equation for bed load sediment. If the actual bed-load transport rate qb is supposed to be the equilibrium one qb*, an equilibrium model of bed-load transport is set up, in which the bed deformation rate is calculated with (Bui and Rutschmann, 2006)

$$(1 - p')\frac{\partial Z_b}{\partial t} + \frac{\partial Q_{bs}}{\partial s} + \frac{\partial Q_{bn}}{\partial n} = 0 \qquad (17)$$

where p' is porosity of the bed material; Q_{bs}, Q_{bn} are bed-load flux in main-flow direction s and cross-flow direction n. They are calculated from the non-equilibrium bed-load equation:

$$\frac{\partial(Q_b\alpha_{bs})}{\partial s} + \frac{\partial(Q_b\alpha_{bn})}{\partial n} = -\frac{1}{L_s}(Q_b - Q_e) \quad (18)$$

where α_{bs}, α_{bn} are direction cosines determining the components of the bed-load transport in the *s* and *n* direction, respectively. This is the mass balance equation for bed-load sediment transport in which all non-equilibrium effects are expressed through the model on the right hand side, assuming the effects to be proportional to the difference between non-equilibrium bed-load Q_b and equilibrium bed-load Q_e and related to the non-equilibrium adaptation length L_s. Both Q_e and L_s are determined from empirical formulae (Bui and Rutschmann, 2006).

In the literature many formulas for equilibrium bed-load transport can be found. Most of them relate bed load transport rate with effective shear stress. In this study, the well-known formula developed by Van Rijn (1984) is applied:

$$Q_e = 0.053(\frac{\rho_s - \rho}{\rho}g)^{0.5}\frac{d_{50}^{1.5}T^{2.1}}{D_*^{0.3}}$$

$$D_* = d_{50}\left[\frac{(\rho_s - \rho)g}{\rho v^2}\right]^{1/3} \qquad (19)$$

$$T = \frac{(U_*')^2 - (U_{*cr})^2}{(U_{*cr})^2}$$

where U_*' is the effective bed shear velocity corresponding to the grain, and U_{*cr} is the critical bed shear velocity for incipient motion given by the Shields diagram.

Generally, the non-equilibrium adaptation length L_s is related to the dimensions of sediment movements, bed forms, and channel geometry. The non-equilibrium adaptation length for bed load may take the value of the average saltation step length of particles or the length of ripples. It is important to mention that, there is no relationship between L_s and L_{drift} (the drift length) as well as L_{lift} (the lift length) described in flow-3d scour model. The first is a horizontal distance, while the others are the vertical ones due to settling of sediment and erosion of the bed.

Phillips and Sutherland (1989) proposed the following equation for the average saltation step length:

$$L_s = \alpha_p(\theta - \theta_{cr})d_{50} \qquad (20)$$

where α_p is constant; θ is Shields parameter. The average saltation step length can also be calculated from an empirical formula of van Rijn (1987):

$$L_s = 3d_{50}D_*^{0.6}T^{0.9} \qquad (21)$$

The bed slope effect was taken into account using the same method proposed by Wu (2004). In this approach, a streamwise component of gravity is added to the bed shear stress without modifying the critical shear stress so that the situation of zero critical shear stress can be avoided.

$$\tau_{be} = \tau_b + \lambda_o\tau_{cr}\sin\phi/\sin\Phi$$

$$\lambda_0 = \begin{cases} 1 & \text{for } \phi \le 0 \\ 1 + 0.22(\tau_b'/\tau_{cr})^{0.15}e^{2\sin\phi/\sin\Phi} & \text{for } \phi \ge 0 \end{cases} \quad (21)$$

In case of steep slope, a sand-slide calculation will be activated at grid point, if there bed slope ϕ is more than repose angle Φ. This sand-slide effect was also previously taken into account in the work of Roulund (2004) and Olsen et al. (1998).

In the computer code FLOW-3D, the flow and sediment transport modules communicate through

a quasi-steady morphodynamic time-stepping mechanism: during the flow computation the bed level is assumed constant and during the computation of the bed level the flow and sediment transport quantities are assumed invariant to the bed level changes. This procedure can be as follows described:

- The bed shear stress calculated from the flow module at each time step is used to calculate the equilibrium bed-load and related parameters.
- Non-equilibrium bed-load is applied for calculation of bed change.
- The effects of the bed change on flow field are taken into account by updating the open volume fraction and the flow field as well as the pressure near the bed as follow:
  1. The change in volume of fluid is equal to the change in bed elevation at this cell.
  2. If the updated volume of fluid is greater than one, this cell will be totally full with fluid (V_f=1.0) and the remaining volume of fluid will be added to the lower cell.
  3. If the updated volume of fluid is less than zero, this cell will be fully blocked (V_f =0.0) and the upper cell will become the boundary cell.
- The fraction areas in x-direction (AFR), y-direction (AFB), and z-direction (AFT) are defined as the average of the volume of fluid of the attached cells.

3 MODEL SETUP

Chatterjee et al. (1994) conducted a series of experiments to study the scour phenomena and sediment transport due to a two-dimensional submerged horizontal jet of water issuing from a sluice and flowing over a rigid apron to an erodible bed. In this paper, RUN-2 was selected for further simulation using FLOW-3D. In this case, the bed material is sand with a mean grain size of 0.76mm, a density of 2,650kg/m^3, bed porosity 0.43, and an angle of repose 29°.
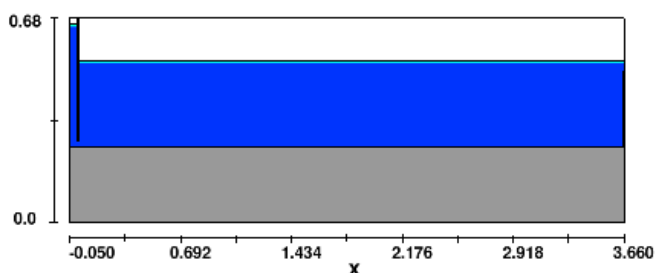

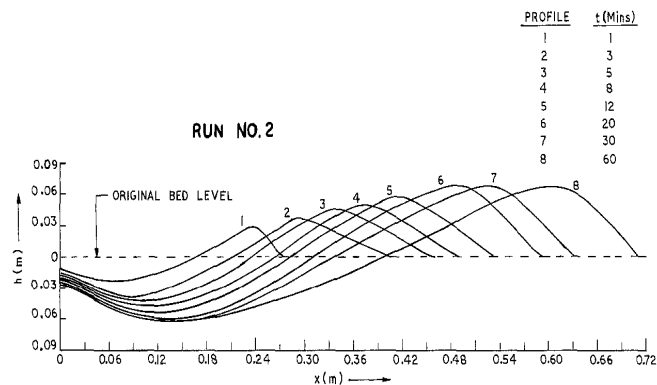Figure 1: Computation domain and initial conditions

Figure 2: Evolution of scour profiles of sand bed in RUN-2 (Chatterjee et al., 1994)

The flow condition for this run is as follows. The apron length is 0.66m and the jet inlet velocity is 1.56m/s. The downstream water depth is controlled to be 0.291m by the outlet weir. In the experiment, the jet inlet velocity is caused by the difference between upstream and downstream water depth. The corresponding water depth difference is 0.118m.

The numerical models were set up based on the experimental conditions of RUN-2 (Fig.1). Calculations started with still water and horizontal bed. At the inlet and outlet boundaries the water elevations are fixed with an assumption of hydrostatic pressure distribution. The top boundary of the domain is the atmosphere and the pressure is set to zero. At the surfaces of objects, wall boundary conditions are used. No-slip condition is set for velocity with zero-normal gradient for pressure. For the turbulence quantities, the wall function is used.

The measured scour profiles along the flume at different times are plotted in Fig.2

4 CALCULATION RESULTS AND DISCUSSIONS

Calculations were firstly carried out by applying the original scour model of FLOW-3D. Using default values for the critical sediment fraction (0.37433) and cohesive sediment fraction (0.3), which were proposed by FLOW-3D for fine sand bed material, the numerical model did not reproduce the scour development with any acceptable quality (Fig.3). Further, a series of calculations with different model parameter sets were done to study their sensitivity on the numerical results. After adjusting model parameters, e.g. using a critical sediment fraction of 0.5, a cohesive sediment fraction of 0.05, an erosion coefficient of 0.05 and a drag coefficient of 1.0, a reasonable agreement between the predicted results and measurements of bed profile, maximum scour depth and maximum deposition after 3 minutes simula-

tion was obtained. However, calculation results for the later stages of scour development were significantly under estimated (Fig.3). While in the experiment the deposition rate increases with time, the predicted deposition rate starts to decrease after about 4 minutes simulation. These results agree with that obtained by Smith (2007).

Further calculations were done using the developed bed-load module. It is clear, when a submerged jet flows over a sediment bed downstream of an apron, the local bed-shear stress induced by the high velocity of the jet exceeds the threshold bed-shear stress for the initiation of sediment motion that results in local scour downstream of the apron. There is no equilibrium sediment transport in this area. With the development of scour hole, the flow depth within the scour hole increases resulting in a reduction of bed-shear stress within the scour hole. Eventually, the equilibrium of scour is attained when the bed-shear stress within the scour hole equals the threshold bed-shear stress for the sediments. From comprehensive studies on the sensitivity to the approaches and parameters used in the morphological model, it was found out that in the case of omitting the non-equilibrium approach (Eq.18), the sediment transport rate at the grid points downstream o the apron was very large, causing an amplification of the resulting errors in the computed bed elevation and sediment transport rate which led to divergence of the computations, thus indicating some interrelation between modeling and numerical effects. After performing test calculations with different formulae for the non-equilibrium adaptation length, the formula of Van Rijn (1987) is chosen in this paper.

Fig.4 shows a comparison between the measured bed profile ater 3 minutes and calculated results of the two models. Using the developed bed-load module, the predicted place of maximun scour agrees well with the measurment. Howerver, the downstream slope of the predicted dune is still over estimated. This could be improved by applying other approaches to considering sand slide effect in the model or taking suspended load for account in the model.
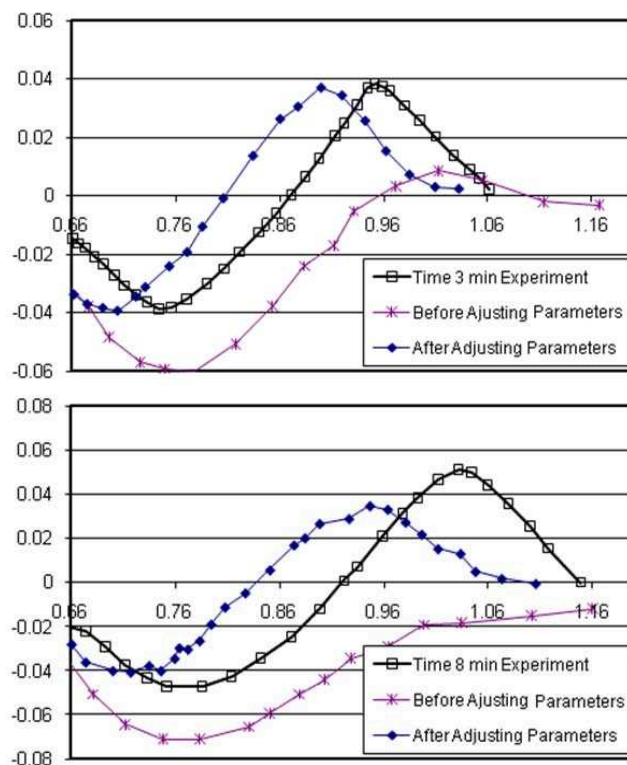

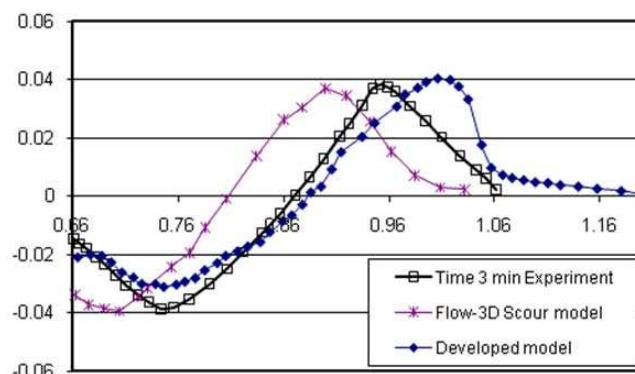Figure 3: Predicted bed profile after different times.

Figure 4: Bed change after 3 minutes.

Figure 5 shows the calculated bed profile and velocity distribution after 3 minutes. One can clearly see from the vector plots that the jet expands and interacts with the bed. In the region above the jet, there is a large scale re-circulating region which extends to downstream. It is important to recognize that this recirculation region provides for a significant downward velocity component downstream of the apron. This fit qualitatively well with the observations made in the experiment.
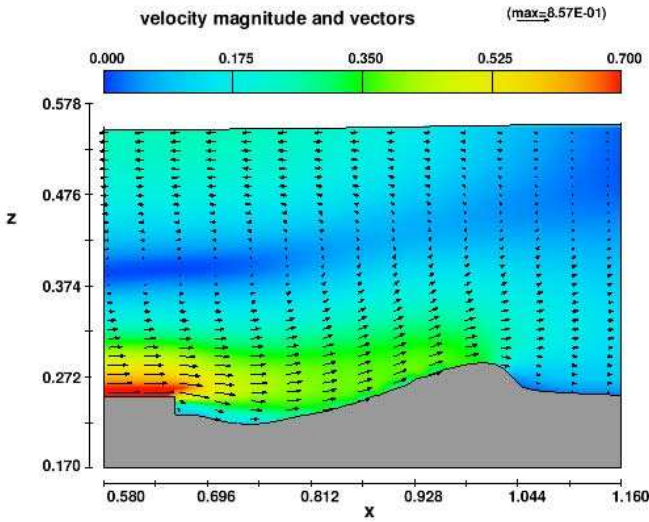
Figure 5: Bed profile and velocity field after 3 minutes

The scour characteristics can be described by the time to reach the equilibrium stage, the locations of the maximum scour depth, and the locations of the peak of the dune from the end of the rigid apron. These characteristics depend on flow parameters and sediment characteristics. Our further purpose is to apply the developed module in FLOW-3D to quantify the relationship of these factors. Hence, model tests were conducted for different efflux discharges q in the flume with the same sand bed material (Tab.1).

Fig.6 shows the bed profile changes after 3 minutes due to the change in flow conditions. It can be seen, by increasing the efflux discharges, the scour process occurs very rapidly. The erosion and deposition rates depend significantly on the flow rates. The peak of the sediment deposition dune moves very quickly downstream, however, the maximum scour position does not change very much. The results agree also with the observations in the experiment. Further calculations for long term simulation of equilibrium scour bed are still under way.

Table 1: Efflux discharges and water depth differences

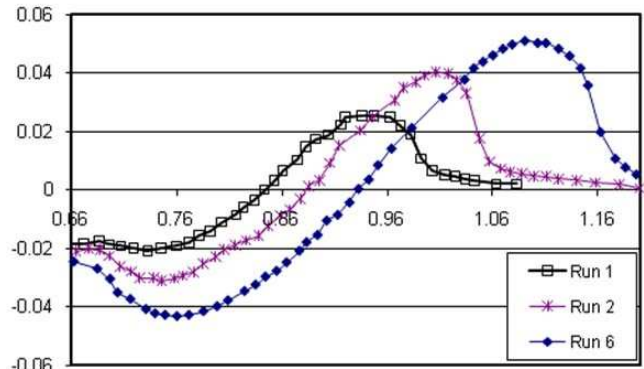| Run number	q (m³/s/m)	Δh (m)
1	0.0159	0.082
2	0.0204	0.118
6	0.0313	0.137

Figure 6: Effect of efflux discharges on bed deformation

5 CONCLUSION

A bed load sediment transport module was integrated into FLOW-3D. The model was tested and validated by simulations for turbulent wall jet scour in a flume. The numerical results were compared with measurements and qualitative observation. Primary good agreement has been obtained using the proposed modeling approach. The maximum scour depth and local scour profile fit well with the experimental data. However the maximum scour depth was lightly under estimated. The slope downstream of the deposition dune was over estimated. The model is used to study the effect of different flow conditions on the bed profile changes. However, further works are needed to enhance the sand slide effect and numerical instability.

NOTATION

The following symbols are used in this paper:

A_i = fractional area open to flow in i direction
a = model constant
d_{50} = median grain size
f_i = viscous accelerations
f_s = solid fraction in computation cell
$f_{s,co}$ = cohesive solid fraction
G_i = body accelerations
k = turbulent kinetic energy
k_s = wall roughness
L_{drift} = drift and settling length scale
L_{lift} = lift length of packed bed
n_s = unit vector normal to bed;
P = pressure
S_{ij} = strain rate tensor
U_i = mean velocity
V_f = fractional volume open to flow
y_o = distance from solid wall to location of tangential velocity
$\tau_{b,i}$ = wall shear stress

τ_{cr} = critical shear stress

ρ = water density

ρ_s = sediment density;

μ_{tot} = total dynamic viscosity

μ = dynamic viscosity

μ_T = eddy viscosity

κ = von Karman constant

ε = turbulent dissipation rate

REFERENCE

Brethour, j., 2003: Modeling Sediment Scour. Flow Science, Inc. Report FSI-03-TN62

Bui, M.D., & Rutschmann, P., 2006: A 3D numerical model of graded sediment transport in non-equilibrium condition. Proc- of the 7th Int. Conf. on Hydroscience and Engineering (ICHE-2006), Philadelphia, USA.

Chatterjee, S. S., Ghosh, S. N., & Chatterjee, M. 1994: Local scour due to submerged horizontal jet. J. Hydraulic Engineering, vol 120(8), 973-992.

Flow Science, Inc. 2008: FLOW-3D User's Manual. Flow Science, Inc.

Hirt, C.W. and Nichols, B.D. (1981) "Volume of Fluid (VOF) Method for the Dynamics of Free Boundaries." J. Computational Physics, Vol. 39, pp 201-225.

Olsen, N. R. B., & Kjellesvig, H. M. 1998:Three- dimensional numerical flow modeling for estimation of maximum local scour. J. of Hydraulic Res., vol 36(4), 579-590

Phillips, B. C., & Sutherland, A. J. 1989: Spatial lag effects in bed load sediment transport. J. of Hydraulic Res., vol 27(1), 115–133.

Roulund, A. 2000: Three- dimensional numerical flow modeling of flow around a bottom mounted pile and its application to scour. Phd thesis, Department of Hydrodynamics and Water Resources, TU Denmark, Series Paper No. 74

Sicilian, J. 1990: A "Favor" based moving obstacle treatment for FLOW-3D. Flow Science, Inc. Internal publication (FSI-90-00-TN24)

Smith,H. D B. 2007: Flow and sediment dynamics around three-dimensional structures in coastal environments. PhD thesis, The Ohio State University.

Smith,H.,& Foster,D. 2005: Modeling of Flow Around a Cylinder Over a Scoured Bed. J. of waterway, port, coastal, and ocean engineering, 10.1061/(ASCE)0733-950X(2005)131:1(14)

Van Rijn, L.C., 1984: Sediment transport, part i:bed load transport. J. Hydraulic Engineering, vol 110(10), 1431-1456

Van Rijn, L.C., 1987: Mathematical modelling of morphological processes in the case of suspended sediment transport. Phd thesis, Faculty of civil engineering, Delft University of technology.

Vasquez, J.A., & Walsh, B. W., 2009: CFD simulation of local scour in complex piers under tidal flow. 33rd IAHR Congress: Water Engineering for a Sustainable Environment. ISBN: 978-94-90365-01-1.

Wu, W., 2004: Depth-Averaged Two-Dimensional Numerical Modeling of Unsteady Flow and Nonuniform Sediment Transport in Open Channels. J. Hydraulic Engineering, vol 130(10), 1013-1024